Electronic Supplementary Material (ESI) for Energy & Environmental Science.

Supplementary Figures and Tables

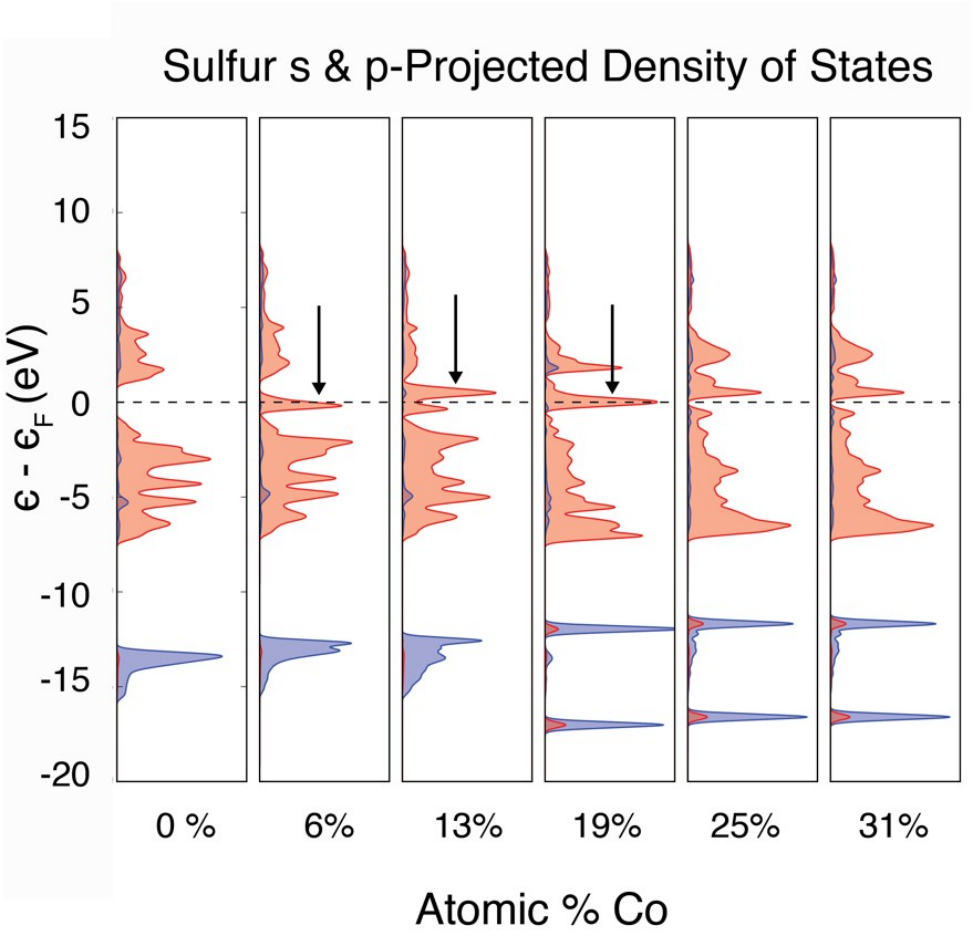

Figure S1. Projected Density of States (PDOS) for S-active Sites on WS_2 Basal Plane

The change in the S-active site density of states with increasing local Co-doping concentration from left to right. The Fermi level is indicated by a black dashed line. Leftmost is the undoped WS_2 surface. Rightmost, a unit cell with 5 Co dopant atoms (corresponding to the surface of 31% Co atomic percentage one). Introducing a metal dopant introduces new states in the p-projected DOS at the Fermi level which can interact with a hydrogen adsorbate. The presence of electronic states near the Fermi level, highlighted with arrows, are correlated with strengthened H-binding energies.

# Co Atoms in Unit Cell	Co atomic percentage	$E_{stability}$ (eV)
0	0%	0.000
1	6%	3.249
2	13%	5.608
3	19%	7.961
4	25%	7.171
5	31%	8.615
6	38%	10.609
7	44%	11.952

Table S1: The formation energies $E_{stability}$ of Co:WS_2. The formation energies $E_{stability}$ is defined as:

$$E_{stability} = (E_{Co\,WS_2} + E_{bulk\,W}) - (E_{WS_2} + E_{bulk\,Co})$$

It describes the energy difference in replacing a metal atom with a dopant (Co), using bulk metal energies as a reference.

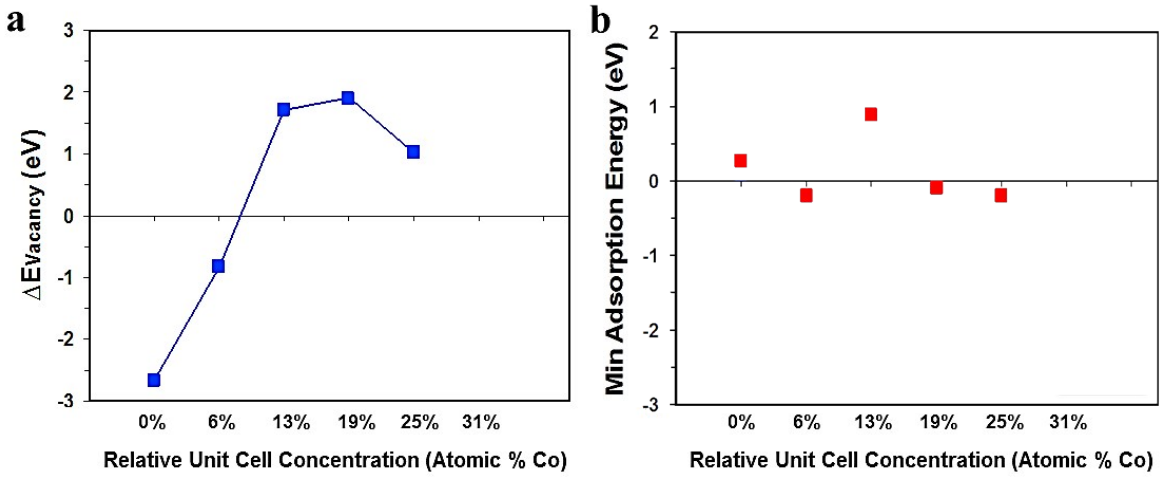

Figure S2. Effect of Co doping concentration on the (a) S-vacancy formation energy and (b) the corresponding minimum $^{\Delta G_H}$ for the basal plane of WS_2. Higher doping concentrations lead to positive values of the vacancy formation energy ($^{\Delta E_{Vacancy}}$), which indicates a more favorable formation process; The H-binding energy to these types of sites is highly variable and dependent on local Co-doping concentration. An S-vacancy with a 19% Co concentration (Co/(Co+W)) ($^{\Delta G_H} = -0.1\ eV$) is the most active surface site, which is comparable to the most active S-sites for the defect-free Co doped 2H-basal plane.

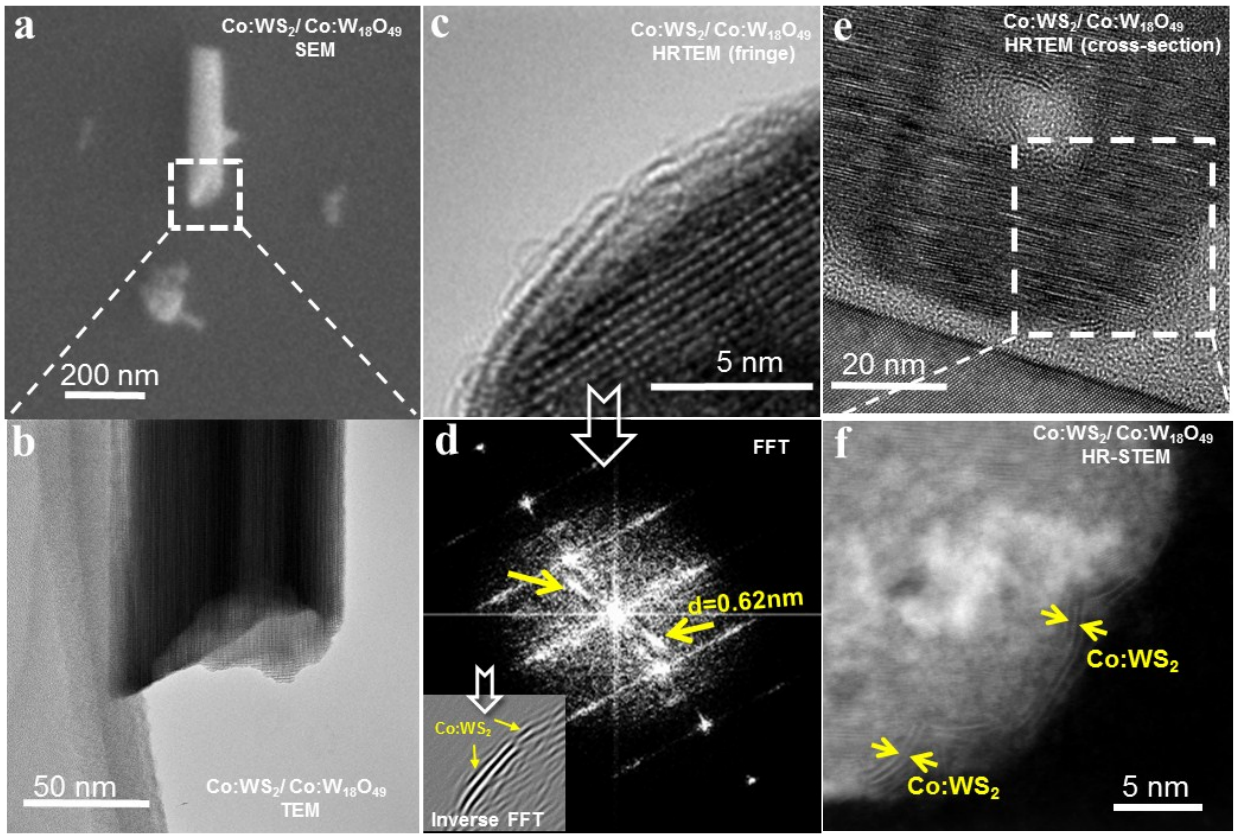

Figure S3. **Additional morphology and crystallinity information of Co:WS_2/Co:$W_{18}O_{49}$ core/shell nanotubes.** (a) SEM and (b) TEM image of a single truncated nanotube. To locate a same nanotube in both SEM and TEM, the truncated nanotube in (a) was first measured by the SEM function of focused ion beam (FIB), and then cut using FIB and transferred to TEM. (c) and (d) are the Fast Fourier transform (FFT) and inversed FFT process, to track the diffraction patterns of Co:WS_2 (002). For this process, first obtain the FFT pattern in (d) from the HRTEM image in (c). From (d) both standard patterns for Co:$W_{18}O_{49}$ and the ones for Co:WS_2 (two points marked in d) are observed. Second cover all points by a mask except for those two associated with the Co:WS_2 signals, and third apply inverse FFT to track the signal for Co:WS_2. The result reveals that the Co:WS_2 signal originates from the several outer layers of the corresponding locations in (c), as marked in the inverse FFT. (e) the HRTEM of the cross section as also illustrated in Figure 3f, to illustrate the position for f. (f) the STEM-HAADF image which shows the fringes of the cross section to clearly track Co:WS_2.

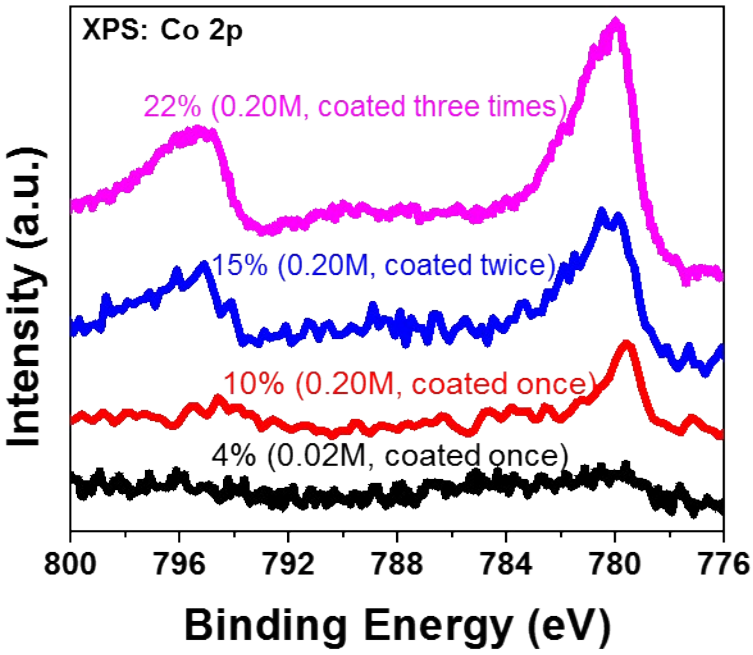

Figure S4. XPS data of Co 2p peaks for Co:WS_2/Co:$W_{18}O_{49}$ core/shell nanotubes prepared with different doping conditions. The percentage represents the surface Co atomic percentage (Co/(Co+W)). The concentration corresponds to the Co precursor concentration for the sol-flame doping process. The coating times correspond to the times of sol-flame doping to increase the surface Co concentration.

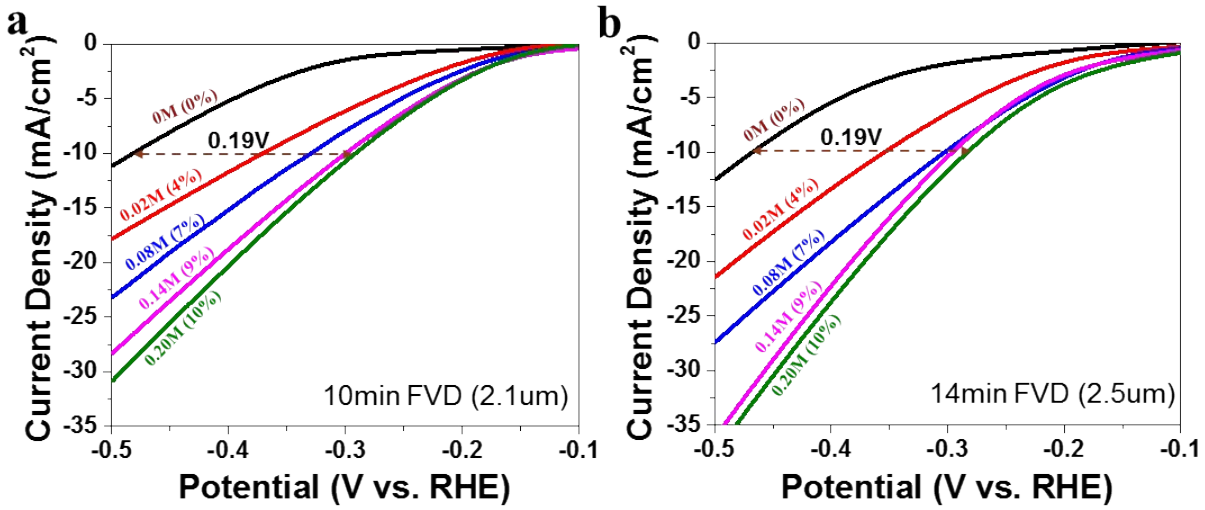

Figure S5. HER activity comparison for Co:WS_2/Co:$W_{18}O_{49}$ core/shell nanotubes prepared with different doping conditions with (a) 10 min and (b) 14 min flame vapor deposition for the nanotube growth. The results show that longer nanotube (*i.e.*, different growth time) leads to higher current density because it is calculated based on the geometric area of FTO. Nevertheless, the nanotube length has little impact on the HER activity improvement (shift of overpotential).

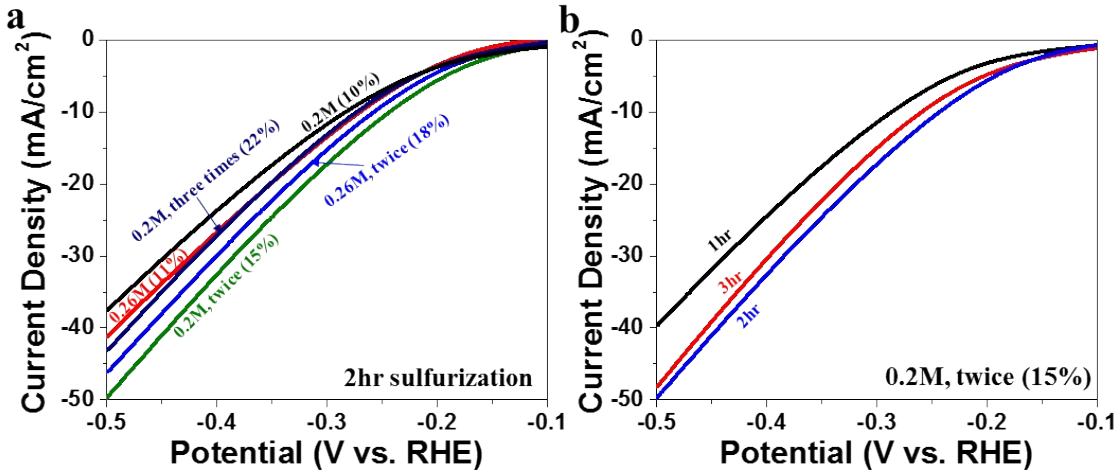

Figure S6. **Additional EC results for different coating times, and WS_2/Co:WS_2/CoS_2.** (a) J-V comparison before iR correction between different coating times of Co doping conditions for the 14mins grown $WS_2/W_{18}O_{49}$ (0.2M, 0.2M coated twice, 0.2M coated three times; 0.26M, 0.26M coated twice). The sulfurization time is 2hr. (b) the performance comparison between different sulfurization time for optimal doping 0.2M, coated twice (15% Co doping).

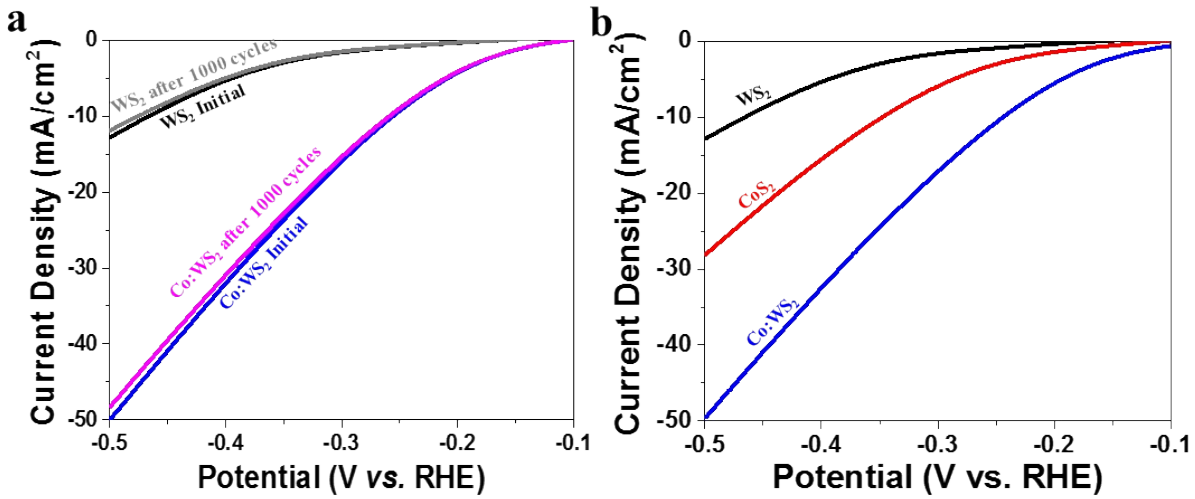

Figure S7. (a) The stability test for both pure WS_2 and optimal doped Co:WS_2, to show the performance between the initial and after 1000 cycles. (b) The J-V curves for WS_2, CoS_2, and Co:WS_2 as different shells on tungsten oxide core.

Catalyst	η_{-10}* before doping	η_{-10}* after doping	η_{-10}* Shift before/after doping	Doping method	Substrate Species
Doping effect for sulfides (Basal plane)					
This work, Co:WS_2	0.45V	0.24V	**0.21V**	Solution-2min flame/quenching	FTO
Zn:MoS_2[19]	0.23	0.14	**0.09V**	hydrothermal	Mix with carbon black on Glassy carbon electrode
Pt:MoS_2[15]	0.21V	0.18V	**0.06V**	Hydrothermal	Glassy carbon rotating disk electrode
Doping effect for sulfides (Edge sites)					
W:MoS_2[47]	0.41V	0.22V	**0.19V**	Hydrothermal/dry;	Glassy carbon electrode
Co:MoS_2[46]	0.26V	0.15V	**0.11V**	Deposition−precipitation	Glassy carbon electrode
Co:FeS_2[48]	0.23V	0.17V	**0.06V**	Wet-chemical sulfurization;	Glassy carbon electrode
WS:N[50]	0.20V	0.14V	**0.06V**	Sol-gel;	Mix with carbon black on Glassy carbon electrode
Fe:NiS_2[49]	0.30V	0.25V	**0.05V**	Hydrothermal/co-sulfurization;	Ti mash
WS:P[51]	0.18V	0.13V	**0.05V**	CVD;	Carbon fiber
Ni:MoS_2[45]	0.35V	0.31V	**0.04V**	Hydrothermal/dry;	Glassy carbon electrode

Table S2. Comparison of element doping effect on the HER overpotential for various sulfides. This table summarizes the recent works that reported doping into varieties of sulfides either into basal plane or edge sites from different approaches. Since some of those work use substrates other than FTO, it is fair to compare the change of η_{-10} before and after doping, rather than its absolute values, to illustrate the doping effect.